

MAKING GW190412: ISOLATED FORMATION OF A 30 + 10 M_⊙ BINARY BLACK-HOLE MERGER

A. OLEJAK¹, K. BELCZYNSKI¹, D. E. HOLZ², J.-P. LASOTA^{1,3}, T. BULIK⁴, M. C. MILLER⁵

¹ Nicolaus Copernicus Astronomical Center, Polish Academy of Sciences, ul. Bartycka 18, 00-716 Warsaw, Poland
(aleksandra.olejak@wp.pl)

² Enrico Fermi Institute, Department of Physics, Department of Astronomy & Astrophysics, KICP, University of Chicago, Chicago, IL 60637, USA

³ Institut d'Astrophysique de Paris, CNRS et Sorbonne Université, UMR 7095, 98bis Bd Arago, 75014 Paris, France

⁴ Astronomical Observatory, Warsaw University, Al. Ujazdowski 4, 00-478 Warsaw, Poland ⁵ Department of Astronomy and Joint Space-Science Institute, University of Maryland, College Park, MD 20742–2421, USA

Draft version May 19, 2022

ABSTRACT

The LIGO/Virgo collaboration has reported the detection of GW190412, a black hole-black hole (BH-BH) merger with the most unequal masses to date: $m_1 = 24.4\text{--}34.7\text{ M}_\odot$ and $m_2 = 7.4\text{--}10.1\text{ M}_\odot$, corresponding to a mass ratio of $q = 0.21\text{--}0.41$ (90% probability range). Additionally, GW190412's effective spin was estimated to be $\chi_{\text{eff}} = 0.14\text{--}0.34$, with the spin of the primary BH in the range $a_{\text{spin}} = 0.17\text{--}0.59$. Based on this and prior detections, $\gtrsim 10\%$ of BH-BH mergers have $q \lesssim 0.4$. Major BH-BH formation channels (i.e., dynamics in dense stellar systems, classical isolated binary evolution, or chemically homogeneous evolution) tend to produce BH-BH mergers with comparable masses (typically with $q \gtrsim 0.5$). Here we test whether the classical isolated binary evolution channel can produce mergers resembling GW190412. We show that our standard binary evolution scenario, with the typical assumptions on input physics we have used in the past, produces such mergers. We provide an explicit example of an unequal mass BH-BH merger, which forms at low metallicity ($Z = 0.002$; $\sim 10\% Z_\odot$) from two massive stars ($M_{\text{ZAMS},1} = 77\text{ M}_\odot$ and $M_{\text{ZAMS},2} = 35\text{ M}_\odot$) and results in a BH-BH merger with $m_1 = 27.0\text{ M}_\odot$, $m_2 = 9.9\text{ M}_\odot$ ($q = 0.37$), with primary black hole spin $a_{\text{spin}} = 0.19$ and an effective spin parameter $\chi_{\text{eff}} = 0.335$. For this particular model of the input physics the overall BH-BH merger rate density in the local Universe ($z \sim 0$) is: $73.5\text{ Gpc}^{-3}\text{ yr}^{-1}$, while for systems with $q < 0.21, 0.28, 0.41$, and 0.59 the rate density is: $0.01, 0.12, 6.8$, and $22.2\text{ Gpc}^{-3}\text{ yr}^{-1}$, respectively. The results from our standard model are consistent with the masses and spins of the black holes in GW190412, as well as with the LIGO/Virgo estimate of the fraction of unequal-mass BH-BH mergers.

Subject headings: stars: black holes, neutron stars, x-ray binaries

1. INTRODUCTION

The first confirmed double black hole (BH-BH) coalescence to be reported from the LIGO/Virgo O3 run, GW190412, differs from all previously announced BH-BH mergers in one important detail: it is the first BH-BH detection that has a mass ratio inconsistent with unity (The LIGO Scientific Collaboration & the Virgo Collaboration 2020). All ten BH-BH mergers announced by the LIGO/Virgo team from the O1 and O2 observational campaigns were consistent with being equal-mass mergers (Abbott et al. 2019a,b; Fishbach & Holz 2020). In contrast, GW190412's component masses are $m_1 = 29.7^{+5.0}_{-5.3}\text{ M}_\odot$ and $m_2 = 8.4^{+1.7}_{-1.0}\text{ M}_\odot$, with a mass ratio of $q = 0.28^{+0.13}_{-0.07}$ (median and 90% symmetric credible interval) and a maximum mass ratio of $q = 0.59$ (99% probability). The dimensionless spin of the primary (more massive) BH spin is estimated to be $a_{\text{spin}} = 0.17\text{--}0.59$, and the BH-BH system effective spin parameter is $\chi_{\text{eff}} = 0.25^{+0.09}_{-0.11}$ (90% probability). The inferred BH-BH merger rate density from O1/O2 is $9.7\text{--}101\text{ Gpc}^{-3}\text{ yr}^{-1}$. From this and previous detections, $\gtrsim 10\%$ of BH-BH mergers have mass ratios $q < 0.40$ (The LIGO Scientific Collaboration & the Virgo Collaboration 2020).

In all major formation channels, BH-BH systems typi-

cally form with comparable-mass components ($q \gtrsim 0.5$). This is the case for the classical isolated binary evolution channel (Bond & Carr 1984; Tutukov & Yungelson 1993; Lipunov et al. 1997; Voss & Tauris 2003; Belczynski et al. 2010b; Dominik et al. 2012; Kinugawa et al. 2014; Hartwig et al. 2016; Spera et al. 2016; Belczynski et al. 2016a; Eldridge & Stanway 2016; Woosley 2016; Stevenson et al. 2017; Kruckow et al. 2018; Hainich et al. 2018; Marchant et al. 2018; Spera et al. 2019; Bavera et al. 2020), the dense stellar system dynamical channel (Portegies Zwart & McMillan 2000; Miller & Hamilton 2002b,a; Portegies Zwart et al. 2004; Gültekin et al. 2004, 2006; O'Leary et al. 2007; Sadowski et al. 2008; Downing et al. 2010; Antonini & Perets 2012; Benacquista & Downing 2013; Bae et al. 2014; Chatterjee et al. 2016; Mapelli 2016; Hurley et al. 2016; Rodriguez et al. 2016; VanLandingham et al. 2016; Askar et al. 2017; Arca-Sedda & Capuzzo-Dolcetta 2017; Samsing 2017; Morawski et al. 2018; Banerjee 2018; Di Carlo et al. 2019; Zevin et al. 2019; Rodriguez et al. 2018; Perna et al. 2019; Kremer et al. 2020), and the chemically homogeneous evolution channel consisting of rapidly spinning stars in isolated binaries (de Mink & Mandel 2016; Mandel & de Mink 2016; Marchant et al. 2016; du Buisson et al. 2020). All of these predictions are challenged by GW190412.

In this study we demonstrate that in the isolated binary channel a small but significant fraction of systems lead to a BH-BH merger similar to GW190412. We provide a proof-of-principle example of an isolated binary that is both qualitatively and quantitatively indistinguishable from GW190412. We emphasize that we have implemented only one model, incorporating our best estimates of the physics and astrophysics which sets the evolution of stars in binary systems. We leave to future work a more extensive study, investigating a greater parameter space and exploring model uncertainties. Our results, when combined and contrasted with similar studies of other formation channels, suggest a plausible origin for GW190412.

2. CALCULATIONS

We use the population synthesis code **StarTrack** (Belczynski et al. 2002, 2008a) to test the possibility of the formation of a BH-BH merger resembling GW190412. We employ the rapid core-collapse supernova (SN) engine NS/BH mass calculation (Fryer et al. 2012), with weak mass loss from pulsational pair instability supernovae (Belczynski et al. 2016c). We assume standard wind losses for massive stars: O/B star Vink et al. (2001) winds and LBV winds (specific prescriptions for these winds are listed in Sec. 2.2 of Belczynski et al. 2010a). We treat accretion onto compact object during Roche lobe overflow (RLOF) and from stellar winds using the analytic approximations presented in King et al. (2001); Mondal et al. (2020), and limit accretion during the common envelope (CE) phase to 5% of the Bondi rate (MacLeod et al. 2017).

The most updated description of **StarTrack** is given in Belczynski et al. (2017). Here we use input physics from model M30 of that paper except for two important differences: First, instead of using the initial mass ratio distribution from Sana et al. (2012), which allows only $q = 0.1$ – 1.0 , we now extend this distribution to lower mass ratios $q = q_{\min}$ – 1.0 , where q_{\min} is chosen in such a way that a star mass is allowed to reach the hydrogen burning limit $M_{\text{ZAMS}} = 0.08 M_{\odot}$. Second, for cases in which we do not know whether we should apply thermal timescale RLOF or CE for systems with NS/BH accretors we use a specific diagnostic diagram to decide between thermal RLOF and CE (see Sec. 5.2 of Belczynski et al. (2008a)). In this single step of binary evolution we previously applied our older numerical approximation of the calculation of accretion onto NS/BH presented in Belczynski et al. (2008b) instead of our newly adopted analytic approach (King et al. 2001; Mondal et al. 2020). These two changes increase the estimated total BH-BH merger rate in the local Universe ($z \sim 0$) from $43.7 \text{ Gpc}^{-3} \text{ yr}^{-1}$ (model M30.B; Belczynski et al. (2017)) to $73.5 \text{ Gpc}^{-3} \text{ yr}^{-1}$ (this study; see below).

3. EXAMPLE OF EVOLUTION

In Figure 1 we present an example of the evolution of a binary system which leads to the formation of close BH-BH system consistent with the parameters estimated for GW190412. This system was picked from the most populated formation channel of BH-BH mergers with $q < 0.41$ (see Tab. 1). This system has both BH masses and primary BH spin a_{spin1} within the range of 90% uncertainties given by The LIGO Scientific Collaboration & the

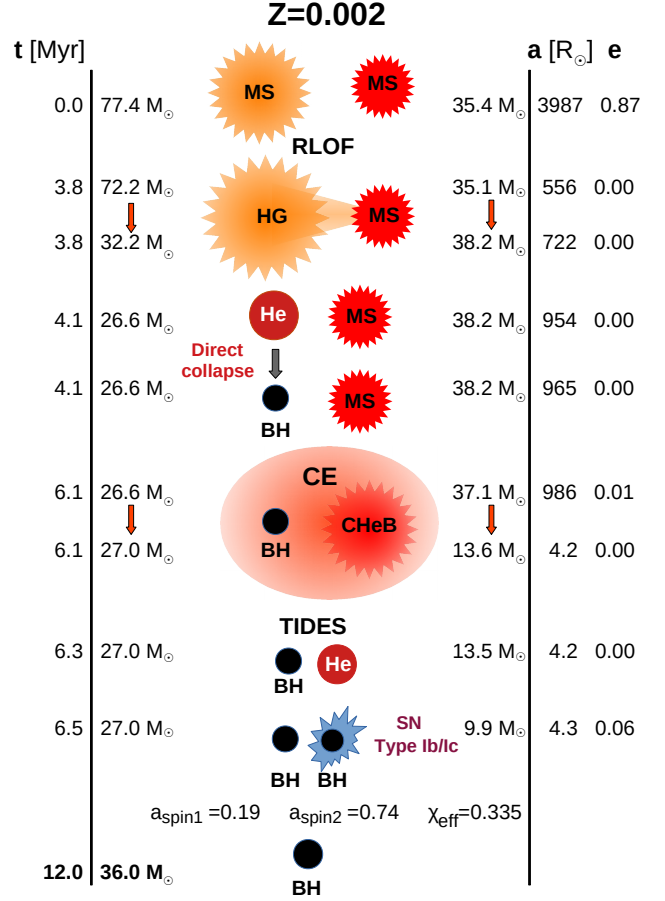


FIG. 1.— Evolution of an isolated binary system that produces a BH-BH merger resembling GW190412 (see Sec. 3 for details). MS: main sequence star, HG: Hertzsprung gap star, CHHeB: core helium burning star, He: naked helium star, BH: black hole, RLOF: Roche lobe overflow, CE: common envelope.

Virgo Collaboration (2020). This system, with initial primary mass $\sim 77 M_{\odot}$ and secondary mass $\sim 35 M_{\odot}$, is formed in a low metallicity environment $Z = 0.002$ ($\sim 0.1 Z_{\odot}$) with an initial separation of $a \sim 4000 R_{\odot}$ and eccentricity $e \sim 0.87$. When the more massive star leaves the main sequence, the system circularizes ($a = 556 R_{\odot}$, $e = 0.0$) at the onset of the stable RLOF phase, during which the donor (primary star) loses a significant amount (over 50%) of its mass. After finishing its nuclear evolution, the primary undergoes direct collapse and forms a first BH with no natal kick and no associated supernova explosion. After the secondary leaves the main sequence and becomes a core helium burning giant, the system enters a CE phase during which the secondary loses its H-rich envelope. The system separation decreases to only $a \sim 4 R_{\odot}$. After CE, the secondary is a massive naked helium star. The binary separation is so small that the secondary is subject to strong tidal interactions and is spun up. At time $t = 6.4$ Myr since the start of the evolution, the secondary explodes as a Type Ib/c supernova (mass ejection of $\sim 2.5 M_{\odot}$; 3D natal kick of $v_{\text{kick}} = 88 \text{ km s}^{-1}$) and forms a second BH. Due to the very small orbital separation, the two BHs, now with a mass ratio of $q = 0.37$, merge in just ~ 5.6

Myr.

The first BH forms with a spin $a_{\text{spin}1} = 0.13$ (calculated from MESA single stellar models with Spruit (1999) angular momentum transport; see Fig. 2 of Belczynski et al. (2017)) that is perfectly aligned with the binary angular momentum ($\theta_1 = 0$ deg). Had we adopted more efficient angular momentum transport in stars (Fuller et al. 2019; Fuller & Ma 2019; Ma & Fuller 2019) than employed in standard MESA then primary BH spin would change to $a_{\text{spin}1} \sim 0.01$. This BH accretes in CE and during stable RLOF from its companion ($\sim 0.4 M_\odot$) and increases its spin to $a_{\text{spin}1} = 0.19$. The second, lower mass, BH forms with spin $a_{\text{spin}2} = 0.74$ that is slightly misaligned by its natal kick to $\theta_2 = 2$ deg. The spin magnitude is obtained from rapidly spinning MESA naked helium star models with spins that correspond to a tidally locked star for a given orbital period in our binary models (see Eq. 15 of Belczynski et al. (2017)). The effective spin parameter of this BH-BH merger is $\chi_{\text{eff}} = 0.335$, within the LIGO/Virgo range for GW190412 (0.14–0.34). It is noted that for the virtually aligned geometry of BH spins with binary angular momentum in this example we do not expect any precession. Yet, there seems to be some evidence for precession in GW190412. Some degree of misalignment would appear in our model if we added for example larger natal kick at the formation of the second BH. At this point binary is so tight that even a large kick would have only small chance to disrupt this binary. The small natal kick applied to the second BH formed through partial fallback is the outcome of our ignorance and simple assumption that natal kicks scale inversely with the amount of the fallback (Fryer et al. 2012). However, little is known about BH natal kicks (Repetto & Nelemans 2015; Mandel 2016; Belczynski et al. 2016b; Repetto et al. 2017; Gandhi et al. 2020).

One might be tempted to identify phase 4 (just before CE in Fig. 1) of the evolution of our binary system with high-mass X-ray binaries of the Cyg X-1 type ($M_{\text{BH}} = 14.8 M_\odot$, O star companion $M_{\text{O}} = 19.2 M_\odot$ and orbital period of $P_{\text{orb}} = 5.6 \text{ d}^1$; this corresponds to a semi-major axis of $a = 43 R_\odot$). However, Cyg X-1 is an active system (it accretes from a wind), which implies an orbital separation that is too tight to allow survival of the subsequent CE phase (Belczynski et al. 2012). If it instead undergoes a stable RLOF (Pavlovskii & Ivanova 2015; Pavlovskii et al. 2017) then the orbit will widen beyond the limit ($a \sim 50 R_\odot$) for two BHs to merge within a Hubble time. We note that BH-BH progenitors in our simulations are initially very wide ($a \gtrsim 1000 R_\odot$) binaries so they can successfully survive the CE phase (de Mink & Belczynski 2015).

4. POPULATION OF LOW- q BH-BH MERGERS

Our simulation results in a $z \sim 0$ population of merging BH-BH systems with a local rate density of $\mathcal{R}_0 = 73.5 \text{ Gpc}^{-3} \text{ yr}^{-1}$. The cumulative distribution of mass ratios for these mergers is presented in Figure 2. In this model the majority of BH-BH mergers ($\sim 80\%$) have large mass ratios ($q > 0.5$), consistent with previous results (Belczynski et al. 2016a). Here we focus on the tail of the distribution extending to more extreme

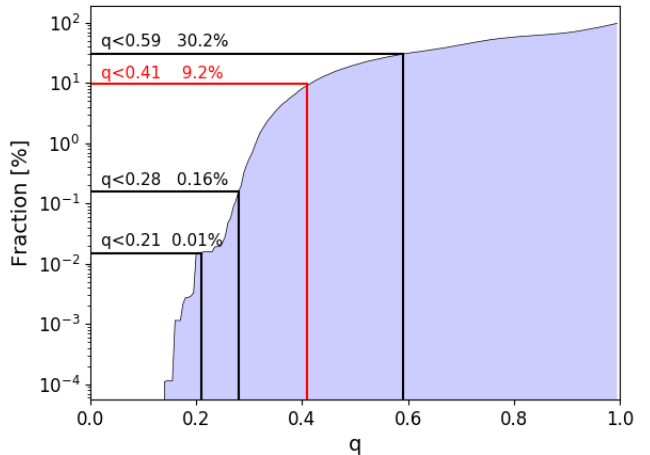


FIG. 2.— Cumulative fraction of merging BH-BH systems with mass ratio smaller than q in the local Universe ($z \sim 0$). Fractions for selected mass ratios $q < 0.21$ (0.01%), $q < 0.28$ (0.16%), and $q < 0.59$ (30.2%) are marked with black lines. The red line marks $q < 0.41$, indicating that 9.2% of our simulated binary mergers at $z \sim 0$ are consistent with the 90% upper limit on q for GW190412.

mass ratios. Our model predicts very few systems with mass ratios smaller than the average value reported for GW190412: 0.16% of binaries have $q < 0.28$. However, we report a more significant fraction of systems with mass ratios smaller than the 90% upper bound on GW190412: 9.2% at $q < 0.41$. This fraction becomes significantly higher for the 99% upper bound on GW190412: 30.2% at $q < 0.59$.

In Table 1 we show evolutionary sequences that lead to the formation of BH-BH mergers with small mass ratios: $q < 0.41$. We list the merger rate density arising for typical evolutionary sequences. These are $z \sim 0$ rate densities and are subpopulations of the overall local BH-BH merger population ($\mathcal{R}_0 = 73.5 \text{ Gpc}^{-3} \text{ yr}^{-1}$). The table presents merger rate densities for BH-BH systems which are increasingly constrained to resemble GW190412:

1. \mathcal{R}_1 : $q < 0.41$,
2. \mathcal{R}_2 : $q < 0.41$ and $24.4 < m_1 / M_\odot < 34.7$ and $7.4 < m_2 / M_\odot < 10.1$,
3. \mathcal{R}_3 : $q < 0.41$ and $24.4 < m_1 / M_\odot < 34.7$ and $7.4 < m_2 / M_\odot < 10.1$ and $0.17 < a_{\text{spin},a} < 0.59$,
4. \mathcal{R}_3 : $q < 0.41$ and $24.4 < m_1 / M_\odot < 34.7$ and $7.4 < m_2 / M_\odot < 10.1$ and $0.17 < a_{\text{spin},a} < 0.59$ and $0.14 < \chi_{\text{eff}} < 0.34$.

The overall rate of systems with $q < 0.41$ is $\mathcal{R}_1 = 6.8 \text{ Gpc}^{-3} \text{ yr}^{-1}$, which corresponds to $\sim 10\%$ of our overall predicted local merger rate density of BH-BH systems ($\mathcal{R}_0 = 73.5 \text{ Gpc}^{-3} \text{ yr}^{-1}$). This is consistent with the LIGO/Virgo estimate of the fraction of low mass ratio systems as inferred from the detection of GW190412 combined with previous detections. We emphasize that Figure 2 shows the distribution of the mass ratios for *all* merging binaries in the local Universe. It does not incorporate gravitational-wave (GW) selection effects, and the GW detected population of binaries will follow a different distribution (e.g. Fishbach et al. 2020). For example,

¹ <https://universeathome.pl/universe/blackholes.php>

TABLE 1
EVOLUTIONARY CHANNELS FOR $q < 0.41$ BH-BH MERGERS

No.	Evolutionary history ^a	\mathcal{R}_1^b	\mathcal{R}_2^c	\mathcal{R}_3^d	\mathcal{R}_4^e
1	RLOF1 BH1 CE2 BH2	5.90	0.49	0.11	0.11
2	RLOF1 BH1 RLOF2 CE2 BH2	0.76	0.04	0.01	0.01
3	RLOF1 BH1 CE2 RLOF2 BH2	0.02	0.01	0.00	0.00
4	OTHER CHANNELS	0.11	0.00	0.01	0.00
	All	6.79	0.54	0.13	0.11

^a: RLOF: stable Roche lobe overflow, CE: common envelope, BH: black hole formation, 1: indicates primary (initially more massive star), 2: secondary star being donor in RLOF or CE.

^b: Merger rate density ($\text{Gpc}^{-3} \text{yr}^{-1}$) for systems with $q < 0.41$.

^c: above and $24.4 < m_1/M_\odot < 34.7$ and $7.4 < m_2/M_\odot < 10.1$.

^d: above and $0.17 < a_{\text{spin},a} < 0.59$.

^e: above and $0.14 < \chi_{\text{eff}} < 0.34$.

current detectors are more sensitive to 30–30 M_\odot than to 30–10 M_\odot binaries, and therefore the detected distributions may de-emphasize lower mass ratio systems. This must be incorporated in detailed model comparisons of mass ratios; the LIGO/Virgo estimate of $\gtrsim 10\%$ of binaries having $q \lesssim 0.4$ is for the true (intrinsic) population, not the detected population.

To produce low mass ratio system with a primary BH as massive as 30 M_\odot a progenitor binary needs to have (i) one very massive component and (ii) a rather extreme initial mass ratio. In addition, the progenitor binary needs to have low metallicity $Z \lesssim 10\% Z_\odot$ ($\lesssim 0.002$) (Belczynski et al. 2010a). There are not many such systems.

5. DISCUSSION AND CONCLUSIONS

The existence of unequal mass binary black holes is to be expected within the isolated binary evolution formation scenario. The mass ratios of such systems were initially investigated by Bulik et al. (2004). They found that in the standard scenario one expects BH-BH systems with high mass ratios above 0.7 to dominate; however, varying the efficiency of the common envelope evolution phase leads to the formation of systems with mass ratios less than 0.5. Although our knowledge of binary evolution and BH-BH formation has subsequently improved, this result appears robust and remains valid. Dominik et al. (2012) have shown the distribution of mass ratios of BH-BH systems in their Figure 9. They find that for subsolar metallicity a significant fraction of these mergers have mass ratio less than 0.5. An additional hint for the existence of unequal mass BH-BH systems from isolated binary evolution comes from the analysis of the future evolution of Cyg X-3 (Belczynski et al. 2013). This system will lead to formation of either a BH-NS or BH-BH binary; in the latter case, the mass ratio is expected to be below 0.6.

The formation channel of GW190412 was considered by Di Carlo et al. (2020), both through dynamical formation in open clusters and through the classical isolated binary evolution channel as discussed here. That group finds that systems like GW190412: “can be matched only by dynamical BBHs born from metal-poor progenitors, because isolated binaries can hardly account for its mass ratio in our models.” Unlike them, we find that systems like GW190412 are naturally formed by isolated binaries in a small but significant fraction of systems. Note also

that the model that we use to account for the formation of GW190412 has also been used to explain the merger rates, masses, and low effective spins of the full O1/O2 LIGO/Virgo BH-BH merger sample (Belczynski et al. 2017).

Mandel & Fragos (2020) have questioned the LIGO/Virgo conclusion that the non-negligible positive effective spin parameter for GW190412 has its origin from a moderate/high spin of the primary (more massive) BH in GW190412 ($a_{\text{spin}1} = 0.17 - 0.59$). Instead, Mandel & Fragos (2020) point out that in the classical isolated binary evolution scenario some second-born BHs may form from tidally spun up helium stars, and that the resulting BHs are expected to have high spins. Using priors consistent with this, they perform an alternate analysis of GW190412 which finds that the primary BH has negligible spin ($a_{\text{spin}1} \sim 0$) while the secondary BH has high spin ($a_{\text{spin}2} = 0.64 - 0.99$). This possibility is also consistent with our results: we find that in $\sim 30\%$ of local BH-BH mergers with $q < 0.41$, tidal interactions are strong enough to produce a lower-mass BH with spin $a_{\text{spin}2} > 0.64$. For example, in Figure 1 we show a system that forms a very close ($a \sim 4 R_\odot$) binary with a BH and a naked helium star (this is the evolutionary phase just prior BH-BH formation). This naked helium star is subject to tidal spin-up, and instead of forming a slowly spinning BH, it forms a rapidly spinning BH ($a_{\text{spin}2} = 0.74$). In contrast with the assumptions of Mandel & Fragos (2020), in our simulations we calculate the spins of primary BHs from single stellar models (Belczynski et al. 2017) and find them to be small, but not negligible. In the particular case shown in Figure 1, the spin of the primary BH is $a_{\text{spin}1} = 0.19$. Since both spins are closely aligned with the binary angular momentum (the secondary is slightly misaligned due to a small natal kick, to $\theta_2 = 2 \text{ deg}$), the effective spin parameter of this system is $\chi_{\text{eff}} = 0.335$, which is consistent with the upper end of the LIGO/Virgo 90% probability estimate for GW190412.

We have shown that the isolated classical binary evolution channel can form binaries similar to GW190412. This is an important explicit proof-of-principle demonstration that the event GW190412 may be the result of isolated evolution. Furthermore, Fig. 2 shows that the detection of a binary with a mass ratio of $q \lesssim 0.4$ is to be expected within the current GW sample, since this sub-population constitutes $\sim 10\%$ of the total population. We find that, if GW190412 formed via the classical isolated binary channel, it likely evolved from a low-metallicity progenitor system with initial mass ratio $q < 0.5$ between the two massive stars, but that otherwise the system followed an evolutionary path that is typical of the majority of BH-BH mergers Belczynski et al. (2016a). Over the coming years the population of GW BH-BH mergers is expected to grow to many hundreds of detections. These will facilitate detailed population studies, including a determination of the distribution of mass ratios. While the existing population of BH-BH mergers can be explained using classical isolated binary evolution, the discovery of a large population of binaries with mass ratio $q < 0.3$ would pose a significant challenge to our models.

KB and AO acknowledge support from the Polish National Science Center (NCN) grant Maestro (2018/30/A/ST9/00050). JPL was supported in part by the French Space Agency CNES. TB was supported by TEAM/2016-3/19 grant from FNP. DEH was supported by NSF grant PHY-1708081, as well as the Kavli

Institute for Cosmological Physics at the University of Chicago through an endowment from the Kavli Foundation. DEH also gratefully acknowledges support from the Marion and Stuart Rice Award. MCM thanks the Radboud Excellence Initiative for supporting his stay at Radboud University.

REFERENCES

- Abbott, B. P., Abbott, R., Abbott, T. D., Abraham, S., LIGO Scientific Collaboration, & Virgo Collaboration. 2019a, *ApJ*, 882, L24
- . 2019b, *Physical Review X*, 9, 031040
- Antonini, F., & Perets, H. B. 2012, *ApJ*, 757, 27
- Arca-Sedda, M., & Capuzzo-Dolcetta, R. 2017, *ArXiv e-prints*
- Askar, A., Szkudlarek, M., Gondek-Rosińska, D., Giersz, M., & Bulik, T. 2017, *MNRAS*, 464, L36
- Bae, Y.-B., Kim, C., & Lee, H. M. 2014, *MNRAS*, 440, 2714
- Banerjee, S. 2018, *MNRAS*, 473, 909
- Bavera, S. S., et al. 2020, *A&A*, 635, A97
- Belczynski, K., Bulik, T., & Fryer, C. L. 2012, *ArXiv e-prints*
- Belczynski, K., Bulik, T., Fryer, C. L., Ruiter, A., Valsecchi, F., Vink, J. S., & Hurley, J. R. 2010a, *ApJ*, 714, 1217
- Belczynski, K., Bulik, T., Mandel, I., Sathyaprakash, B. S., Zdziarski, A. A., & Mikołajewska, J. 2013, *ApJ*, 764, 96
- Belczynski, K., Dominik, M., Bulik, T., O’Shaughnessy, R., Fryer, C. L., & Holz, D. E. 2010b, *ApJ*, 715, L138
- Belczynski, K., Holz, D. E., Bulik, T., & O’Shaughnessy, R. 2016a, *Nature*, 534, 512
- Belczynski, K., Kalogera, V., & Bulik, T. 2002, *ApJ*, 572, 407
- Belczynski, K., Kalogera, V., Rasio, F. A., Taam, R. E., Zezas, A., Bulik, T., Maccarone, T. J., & Ivanova, N. 2008a, *ApJS*, 174, 223
- Belczynski, K., Repetto, S., Holz, D. E., O’Shaughnessy, R., Bulik, T., Berti, E., Fryer, C., & Dominik, M. 2016b, *ApJ*, 819, 108
- Belczynski, K., Taam, R. E., Rantsiou, E., & van der Sluys, M. 2008b, *ApJ*, 682, 474
- Belczynski, K., et al. 2016c, *A&A*, 594, A97
- . 2017, *arXiv e-prints*, arXiv:1706.07053
- Benacquista, M. J., & Downing, J. M. B. 2013, *Living Reviews in Relativity*, 16, 4
- Bond, J. R., & Carr, B. J. 1984, *MNRAS*, 207, 585
- Bulik, T., Gondek-Rosińska, D., & Belczynski, K. 2004, *MNRAS*, 352, 1372
- Chatterjee, S., Rodriguez, C. L., Kalogera, V., & Rasio, F. A. 2016, *ArXiv e-prints*
- de Mink, S. E., & Belczynski, K. 2015, *ApJ*, 814, 58
- de Mink, S. E., & Mandel, I. 2016, *MNRAS*, 460, 3545
- Di Carlo, U. N., Giacobbo, N., Mapelli, M., Pasquato, M., Spera, M., Wang, L., & Haardt, F. 2019, *arXiv e-prints*
- Di Carlo, U. N., et al. 2020, *arXiv e-prints*, arXiv:2004.09525
- Dominik, M., Belczynski, K., Fryer, C., Holz, D., Berti, B., Bulik, T., Mandel, I., & O’Shaughnessy, R. 2012, *ApJ*, 759, 52
- Downing, J. M. B., Benacquista, M. J., Giersz, M., & Spurzem, R. 2010, *MNRAS*, 407, 1946
- du Buisson, L., et al. 2020, *arXiv e-prints*, arXiv:2002.11630
- Eldridge, J. J., & Stanway, E. R. 2016, *MNRAS*, 462, 3302
- Fishbach, M., Farr, W. M., & Holz, D. E. 2020, *ApJ*, 891, L31
- Fishbach, M., & Holz, D. E. 2020, *ApJ*, 891, L27
- Fryer, C. L., Belczynski, K., Wiktorowicz, G., Dominik, M., Kalogera, V., & Holz, D. E. 2012, *ApJ*, 749, 91
- Fuller, J., & Ma, L. 2019, *ApJ*, 881, L1
- Fuller, J., Piro, A. L., & Jermyn, A. S. 2019, *MNRAS*
- Gandhi, P., Rao, A., Charles, P. A., Belczynski, K., Maccarone, T. J., Arur, K., & Corral-Santana, J. M. 2020, *arXiv e-prints*, arXiv:2002.00871
- Gültekin, K., Miller, M. C., & Hamilton, D. P. 2004, *ApJ*, 616, 221
- . 2006, *ApJ*, 640, 156
- Hainich, R., et al. 2018, *A&A*, 609, A94
- Hartwig, T., Volonteri, M., Bromm, V., Klessen, R. S., Barausse, E., Magg, M., & Stacy, A. 2016, *MNRAS*, 460, L74
- Hurley, J. R., Sippel, A. C., Tout, C. A., & Aarseth, S. J. 2016, *MNRAS*, 33, e036
- King, A. R., Davies, M. B., Ward, M. J., Fabbiano, G., & Elvis, M. 2001, *ApJ*, 552, L109
- Kinugawa, T., Inayoshi, K., Hotokezaka, K., Nakauchi, D., & Nakamura, T. 2014, *MNRAS*, 442, 2963
- Kremer, K., et al. 2020, *ApJS*, 247, 48
- Kruckow, M. U., Tauris, T. M., Langer, N., Kramer, M., & Izzard, R. G. 2018, *ArXiv e-prints*
- Lipunov, V. M., Postnov, K. A., & Prokhorov, M. E. 1997, *Astronomy Letters*, 23, 492
- Ma, L., & Fuller, J. 2019, *arXiv e-prints*
- MacLeod, M., Antoni, A., Murguía-Berthier, A., Macias, P., & Ramirez-Ruiz, E. 2017, *ApJ*, 838, 56
- Mandel, I. 2016, *MNRAS*, 456, 578
- Mandel, I., & de Mink, S. E. 2016, *MNRAS*, 458, 2634
- Mandel, I., & Fragos, T. 2020, *arXiv e-prints*, arXiv:2004.09288
- Mapelli, M. 2016, *MNRAS*, 459, 3432
- Marchant, P., Langer, N., Podsiadlowski, P., Tauris, T. M., & Moriya, T. J. 2016, *A&A*, 588, A50
- Marchant, P., Renzo, M., Farmer, R., Pappas, K. M. W., Taam, R. E., de Mink, S., & Kalogera, V. 2018, *arXiv e-prints*
- Miller, M. C., & Hamilton, D. P. 2002a, *ApJ*, 576, 894
- . 2002b, *MNRAS*, 330, 232
- Mondal, S., Belczynski, K., Wiktorowicz, G., Lasota, J.-P., & King, A. R. 2020, *MNRAS*, 491, 2747
- Morawski, J., Giersz, M., Askar, A., & Belczynski, K. 2018, *ArXiv e-prints*
- O’Leary, R. M., O’Shaughnessy, R., & Rasio, F. A. 2007, *Phys. Rev. D*, 76, 061504
- Pavlovskii, K., & Ivanova, N. 2015, *MNRAS*, 449, 4415
- Pavlovskii, K., Ivanova, N., Belczynski, K., & Van, K. X. 2017, *MNRAS*, 465, 2092
- Perna, R., Wang, Y.-H., Farr, W. M., Leigh, N., & Cantiello, M. 2019, *ApJ*, 878, L1
- Portegies Zwart, S. F., Baumgardt, H., Hut, P., Makino, J., & McMillan, S. L. W. 2004, *Nature*, 428, 724
- Portegies Zwart, S. F., & McMillan, S. L. W. 2000, *ApJ*, 528, L17
- Repetto, S., Igoshev, A. P., & Nelemans, G. 2017, *MNRAS*, 467, 298
- Repetto, S., & Nelemans, G. 2015, *MNRAS*, 453, 3341
- Rodriguez, C. L., Amaro-Seoane, P., Chatterjee, S., Kremer, K., Rasio, F. A., Samsing, J., Ye, C. S., & Zevin, M. 2018, *Phys. Rev. D*, 98, 123005
- Rodriguez, C. L., Haster, C.-J., Chatterjee, S., Kalogera, V., & Rasio, F. A. 2016, *ApJ*, 824, L8
- Sadowski, A., Belczynski, K., Bulik, T., Ivanova, N., Rasio, F. A., & O’Shaughnessy, R. 2008, *ApJ*, 676, 1162
- Samsing, J. 2017, *ArXiv e-prints*
- Sana, H., et al. 2012, *Science*, 337, 444
- Spera, M., Giacobbo, N., & Mapelli, M. 2016, *Mem. Soc. Astron. Italiana*, 87, 575
- Spera, M., Mapelli, M., Giacobbo, N., Trani, A. A., Bressan, A., & Costa, G. 2019, *MNRAS*, 485, 889
- Spruit, H. C. 1999, *A&A*, 349, 189
- Stevenson, S., Vigna-Gómez, A., Mandel, I., Barrett, J. W., Neijssel, C. J., Perkins, D., & de Mink, S. E. 2017, *Nature Communications*, 8, 14906
- The LIGO Scientific Collaboration, & the Virgo Collaboration. 2020, *arXiv e-prints*, arXiv:2004.08342
- Tutukov, A. V., & Yungelson, L. R. 1993, *MNRAS*, 260, 675
- VanLandingham, J. H., Miller, M. C., Hamilton, D. P., & Richardson, D. C. 2016, *ApJ*, 828, 77
- Vink, J. S., de Koter, A., & Lamers, H. J. G. L. M. 2001, *A&A*, 369, 574
- Voss, R., & Tauris, T. M. 2003, *MNRAS*, 342, 1169
- Woosley, S. E. 2016, *ApJ*, 824, L10
- Zevin, M., Samsing, J., Rodriguez, C., Haster, C.-J., & Ramirez-Ruiz, E. 2019, *ApJ*, 871, 91